TOPICAL REVIEW — Topological electronic states

Quantum transport properties of the three-dimensional Dirac semimetal Cd_3As_2 single crystals*

Lan-Po He(何兰坡)[1] and Shi-Yan Li(李世燕)[1,2,†]

[1] State Key Laboratory of Surface Physics, Department of Physics, and Laboratory of Advanced Materials, Fudan University, Shanghai 200433, China
[2] Collaborative Innovation Center of Advanced Microstructures, Nanjing 210093, China

(Received 4 September 2016; revised manuscript received 20 October 2016; published online 26 October 2016)

The discovery of the three-dimensional Dirac semimetals have expanded the family of topological materials, and attracted massive attentions in recent few years. In this short review, we briefly overview the quantum transport properties of a well-studied three-dimensional Dirac semimetal, Cd_3As_2. These unusual transport phenomena include the unexpected ultra-high charge mobility, large linear magnetoresistivity, remarkable Shubnikov–de Hass oscillations, and the evolution of the nontrivial Berry's phase. These quantum transport properties not only reflect the novel electronic structure of Dirac semimetals, but also give the possibilities for their future device applications.

Keywords: three-dimensional Dirac semimetal, linear magnetoresistance, Shubnikov–de Hass oscillations, Berry's phase

PACS: 71.20.–b, 71.55.Ak, 71.70.Di, 72.15.Gd **DOI:** 10.1088/1674-1056/25/11/117105

1. Introduction

Two-dimensional (2D) Dirac electron systems, represented by graphene and the surface state of three-dimensional (3D) topological insulators (TIs), exhibit exotic quantum phenomena and have been considered as one of the central topics in modern condensed matter physics.[1–4] Recently, 3D Dirac semimetal (DSM) has been proposed as another new class of topological material,[5–8] and caught plenty of attention quickly. This new kind of topological material can be regarded as a 3D analog of graphene because it possesses 3D gapless Dirac points (at Fermi level) in the bulk Brillouin zone, whose low-energy physics can be effectively described as four-component Dirac fermions,

$$\boldsymbol{H} = \begin{pmatrix} \upsilon\boldsymbol{\sigma}\cdot\boldsymbol{k} & 0 \\ 0 & -\upsilon\boldsymbol{\sigma}\cdot\boldsymbol{k} \end{pmatrix}, \tag{1}$$

where $\boldsymbol{\sigma}$ is the Pauli matrix, $\boldsymbol{k}$ is the crystal moment, and υ is the velocity.[5–9] This is different from that of 3D Weyl semimetal (WSM), in which the low-energy physics is given as two-component Weyl fermions $\boldsymbol{H} = \upsilon\boldsymbol{\sigma}\cdot\boldsymbol{k}$ around Weyl points.[5–9] Therefore, when additional symmetry (e.g., crystalline symmetry) is present to protect the 3D Dirac point, a Dirac point could be viewed as overlapping of two distinct Weyl points. Otherwise, two Weyl nodes with opposite chirality would annihilate each other if they overlap in momentum space, and open up a gap.[5,6,8] In 3D DSM, in the presence of time reversal symmetry and inversion symmetry, a pair of 3D Dirac points is formed at the crossing of two doubly degenerate bands on a high-symmetry axis, which are protected by crystalline symmetry.[5–8] Breaking symmetry in DSM is a simple way to accessing the exotic WSM.[5,6,10] Furthermore, DSM may host a surface Fermi loop.[6,8,10–12] It is composed of two half-circle Fermi arcs touching at the singularity points, where the surface projection of bulk Dirac points exist.[5,6] This contrasts sharply with a surface Fermi arc in WSM, because of the different topological origin.[5,6,13]

Theoretically, several materials have been proposed as candidates for DSM, such as BiO_2, A_3Bi (A = Na, K, Rb), Cd_3As_2, and some distorted spinels.[5–7,14] Many unusual phenomena were also predicted, such as the giant diamagnetism which diverges logarithmically when the Fermi energy approaches the 3D Dirac point;[5,15] quantum linear magnetoresistance even up to room temperature and large negative magnetoresistance due to the novel bulk band structure;[5,6,16–21] the quantum spin Hall effect in its quantum-well structure;[5,22] and possible topological superconductivity when doping carriers.[6,12,23,24] Soon after these theoretical predictions, the angle-resolved photoemission spectroscopy (ARPES) experiments were performed on Na_3Bi and Cd_3As_2 single crystals and two bulk 3D Dirac points were observed on the opposite sides of the Brillouin zone center point Γ along k_z.[25–29] Scanning tunneling microscopy (STM) experiments also support the existence of 3D Dirac points in Cd_3As_2 single crystals.[30] Later, the distinct surface states of both two compounds were re-

*Project supported by the National Basic Research Program of China (Grant Nos. 2012CB821402 and 2015CB921401), the National Natural Science Foundation of China, the Program for Professor of Special Appointment (Eastern Scholar) at Shanghai Institutions of Higher Learning, and STCSM of China (Grant No. 15XD1500200).

†Corresponding author. E-mail: shiyan_li@fudan.edu.cn

© 2016 Chinese Physical Society and IOP Publishing Ltd

vealed by ARPES measuremens.[11,31] More recently, the point contact experiments have shown a hint of topological superconductivity under the tip in both Cd_3As_2 single crystals and polycrystals.[32,33] Pressure-induced superconductivity was also observed in Cd_3As_2 by high-pressure resistance measurements.[34] The magneto-transport measurements on Cd_3As_2 nano-structures have discovered a large negative magnetoresistance, which was attributed to the chiral anomaly.[35,36] Moreover, due to the large surface-to-volume ratio in nano-structures, the Aharonov–Bohm oscillations have been detected in individual single-crystalline Cd_3As_2 nanowires.[37]

The quantum transport measurement is an important tool to detect the unusual band structure of 3D DSMs. Following those theoretical predictions, a lot of quantum transport studies were carried out on Na_3Bi and Cd_3As_2 single crystals, and many interesting transport phenomena were observed.[38–47] Considering that Cd_3As_2 is far more stable in air than Na_3Bi, the Cd_3As_2 single crystal is more suitable for transport measurements. In this short review, we will summarize these quantum transport properties of Cd_3As_2 single crystals.

2. Quantum transport properties

2.1. Crystal and band structure

The standard method of growing Cd_3As_2 single crystals is using Cd flux with the starting composition Cd : As = 8 : 3, as described in Refs. [38] and [48]. The typical size of as-grown Cd_3As_2 single crystals is several millimeters. This method usually gives Cd_3As_2 single crystals with large natural (112) surface. It is also convenient to employ vapor transport method to grow Cd_3As_2 single crystals with large natural (001) surface.[46,49,50] At ambient pressure, Cd_3As_2 has a distorted superstructure of the antifluorite structure type with a tetragonal unit cell of $a = 12.633(3)$ Å and $c = 25.427(7)$ Å in the centrosymmetric $I4_1/acd$ space group,[48] which is shown in Fig. 1(a). Note that in the first theoretical paper predicting Cd_3As_2 to be DSM,[6] one of the two crystal structures from early experiment[51] is non-centrosymmetric and the four-fold Dirac nodes are protected by proper uniaxial rotational symmetry instead of inversion symmetry. Ali *et al.* reinvestigated the crystal structure by single-crystal x-ray diffraction and pointed this out.[48] They calculated the electronic structure using the experimentally determined centrosymmetric structure and found that the band structure is similar to the non-centrosymmetric one.[48] The overall structure of Cd_3As_2 in Fig. 1(a) can be viewed as a $2 \times 2 \times 4$ superstructure stacked from the small cubic sub-cell shown in Fig. 1(b),[48] in which the cubic Cd lattice with two vacancies resides in a face-centered cubic As lattice.

Figure 1(c) shows the calculated electronic structure of Cd_3As_2 from the crystal structure shown in Figs. 1(a) and 1(b). The bulk conduction band (contributed by Cd 5s states) and valence band (contributed by As 4p states) cross at a discrete point (i.e., Dirac point) along Γ–Z direction at the Fermi level. In the presence of C_4 rotational symmetry and time-reversal symmetry, the 3D Dirac point in Cd_3As_2 is 4-fold degenerate at the Fermi level.[48] The bulk Brillouin zone of Cd_3As_2 is plotted in Fig. 1(d), in which two Dirac points locate on the opposite sides of the Brillouin zone center point Γ along the k_z direction. Moreover, according to Fig. 1(c), there are no other additional trivial bands crossing the Fermi level, which means the Fermi surface of Cd_3As_2 only consists of 3D Dirac points. Therefore, the transport properties are only dominated by 3D Dirac fermions. As mentioned above, Cd_3As_2 is very stable in air, unlike Na_3Bi. Therefore, Cd_3As_2 is an ideal system to investigate the quantum transport properties of DSM.

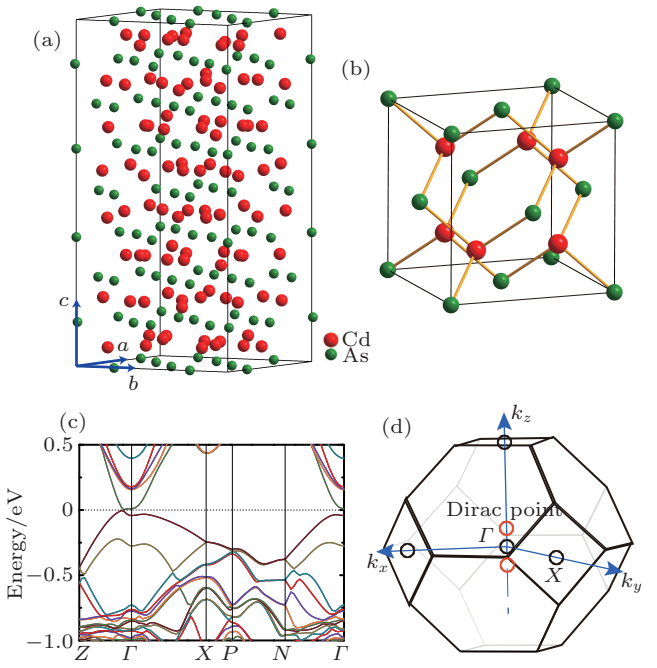


Fig. 1. (color online) (a) The crystal structure of Cd_3As_2, which has a distorted superstructure of the antifluorite structure type with a tetragonal unit cell in the cetrosymmetric $I4_1/acd$ space group. (b) A small sub-cell of the overall structure of Cd_3As_2, in which the cubic Cd lattice with two vacancies resides in a face-centered cubic As lattice. The overall structure of Cd_3As_2 can be viewed as a $2 \times 2 \times 4$ superstructure stacked from it. (c) The calculated electronic structure of Cd_3As_2. A band crossing merges along Γ–Z at the Fermi level, representative of Dirac point. (d) Bulk Brillouin zone of Cd_3As_2. Two 3D Dirac points (red dots) locate on the opposite sides of the Brillouin zone center point Γ along k_z direction.

2.2. Ultra-high charge mobility and linear magnetoresistivity

Cd_3As_2 is a well-known compound which has been studied for decades.[52–54] The typical temperature dependence of the longitudinal resistivity of Cd_3As_2 single crystals at zero magnetic field shows a metallic behavior, with the carrier concentration n_e varying from $\sim 10^{16}$ to $\sim 10^{18}$ cm^{-3}. Considering the different qualitity of Cd_3As_2 single crystals, the resid-

ual resistivity ρ_0 could vary from $\sim$ 10 nΩ·cm to 10 $\mu\Omega$·cm with the residual resistivity ratio (RRR) ranging from $\sim$ 5 to $\sim$ 1000 (Table 1). The high charge mobility ($\sim 10^4$ cm^2/Vs) in Cd_3As_2 has been known from early transport studies.[53,54] Surprisingly, Liang *et al.* discovered an unexpected ultra-high charge mobility (as high as 9×10^6 cm^2/Vs at 5 K) in some Cd_3As_2 single crystals, which is shown in Fig. 2.[39] Actually, they found that there are two kinds of single crystals which were named as "Set A" (single domain) and "Set B" (multidomain) samples. The ultra-high charge mobility exists in "Set A" samples with very low residual resistivity (21 nΩ·cm) and very high RRR (4100) (Table 1). They proposed a protection mechanism that strongly suppress backscattering in zero magnetic field,[39] and this protection results in the ultra-high mobility. Later, this kind of Cd_3As_2 single crystal with ultra-high mobility was also investigated by Zhao *et al.*[42]

Table 1. The parameters of transport properties, including residual resistivity ρ_0, residual resistivity ratio (RRR), carrier concentration n_e, mobility μ, cyclotron mass m^*, Fermi velocity v_F, and Fermi vector k_F.

Ref.	ρ_0 /$\mu\Omega$·cm	RRR	n_e /10^{18} cm^{-3}	μ /10^4 cm^2/Vs	m^*/m_e	v_F /10^6 m·s^{-1}	k_F /Å^{-1}
[38]	28.2	5.7	5.3	4.1	0.044	1.1	0.042
[39]	32.2	7.3	15	2	0.094	0.93	0.076
[39]	0.021	4100	7.4	870	–	–	–
[40]	$\sim$ 2000	$\sim$ 2	0.05	6.5	0.025	0.92	0.02
[41]	42	$\sim$ 4	1.8	8	0.023	1.54	0.031

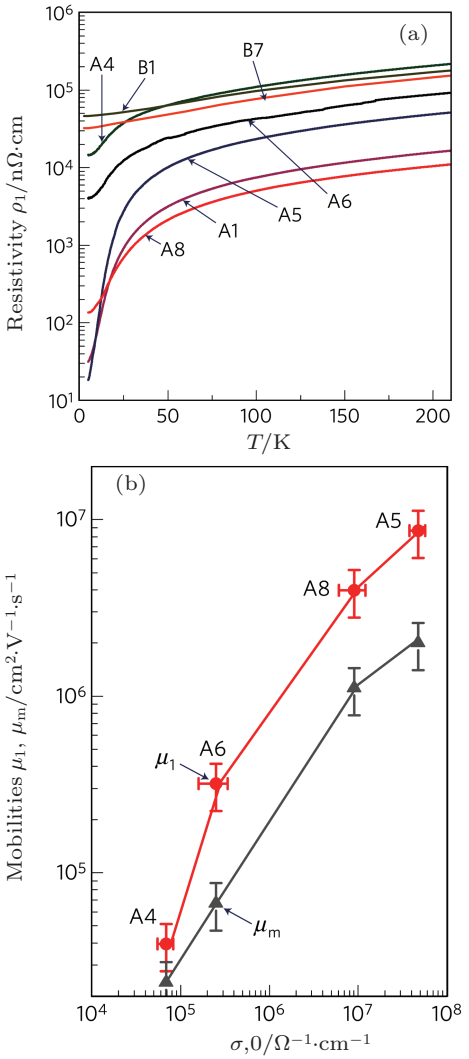


Fig. 2. (color online) (a) Curves of the resistivity versus temperature measured along the needle axis in five "Set A" and two "Set B" samples (semilog scale).[39] (b) Measured mobility versus the zero field conductivity for Set A samples (A4, A5, A6, and A8).[39]

The first magnetotransport study of Cd_3As_2 single crystals after the theoretical prediction was reported by He *et al.*[38] The single crystals used in that work were grown in Cd flux, with $\rho_0 = 28.2$ $\mu\Omega$ cm and RRR $\approx$ 5.7. Figure 3 shows the longitudinal magnetoresistance (MR) at various temperatures, with the magnetic field perpendicular to the (112) plane.[38] The MR is defined by MR $= (R_{xx}(B) - R_{xx}(0\ \mathrm{T}))/R_{xx}(0\ \mathrm{T}) \times 100\%$. Firstly, one can see that the MR shows no sign of saturation with magnetic field up to 14.5 T even near room temperature (280 K). Secondly, with decreasing temperature, the MR increases dramatically and oscillates remarkably. At 1.5 K, a large MR up to $\sim$ 1600% was observed in a field of 14.5 T and the oscillations can be tracked down to a field as low as $B \approx 2$ T which reflects the high mobility in Cd_3As_2.

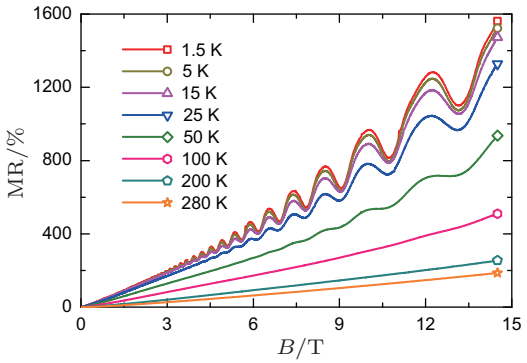


Fig. 3. (color online) The longitudinal magnetoresistance (MR) of Cd_3As_2 single crystal at various temperatures with the field perpendicular to the (112) plane.[38] The MR presents remarkable oscillations at low temperatures and unusual linear behavior even near room temperature.

At 280 K, the MR reaches as high as 200% at 14.5 T and shows a quite linear behavior above 3 T, which is consistent with the theoretical prediction.[6] This unusual linear MR has been observed by other transport works as well.[39–41] Usually there are two scenarios to explain the linear MR: a) the quantum limit scenario[16,17] and b) the classical disorder scenario.[55–57] For the former one, in the presence of linear energy dispersion, linear MR could be achieved when all of the carriers occupy the lowest Landau level (quantum limit);[16,17] for the latter one, linear MR arises because the local current density acquires spatial fluctuations in both magnitude and direction, as a result of the heterogeneity or microstructure caused by nonhomogeneous carrier and mobility

distribution.[55–57] Both scenarios have been used to successfully explain the linear MR observed in some materials.[55–60]

Wang *et al.* proposed that Cd_3As_2 can support sizable quantum linear MR even up to room temperature at the quantum limit due to its linear energy dispersion.[6] However, this requirement is actually not satisfied in the field range, since there is clearly more than one Landau levels occupied, as will be seen in Fig. 4(a). Similar situations have also occurred in other transport works.[39–41] Liang *et al.* and Feng *et al.* suggested that the linear MR in Cd_3As_2 single crystals may relate to the field-induced change to the Fermi surface,[39,40] since the Dirac–Fermi surface would split into two Weyl–Fermi surfaces due to time-reversal symmetry breaking under magnetic fields.[40] However, Narayanan *et al.* performed magneto-transport measurements of Cd_3As_2 single crystals with linear MR in magnetic fields up to 65 T (approaching the quantum limit) and found no additional frequencies (only spin splitting due to the large g factors) or changes in scattering.[4] Therefore, they proposed that the unconventional linear MR is likely caused by disorder effects, as it scales with the high mobility rather than directly linked to Fermi surface changes.[41] Note that quantum linear MR has been observed in Cd_3As_2 single crystals at low temperature by Zhao *et al.*, in which the linear MR appeared after reaching the quantum limit (about 43 T in their samples).[42]

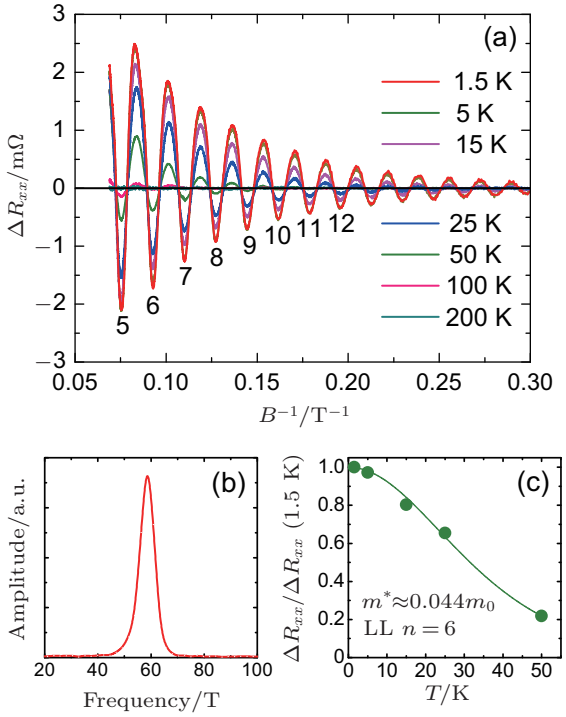


Fig. 4. (color online) (a) The oscillatory component ΔR_{xx}, extracted from R_{xx} by subtracting a smooth background, as a function of $1/B$ at various temperatures for Cd_3As_2 single crystal.[38] (b) Fast Fourier transform (FFT) of the oscillatory component ΔR_{xx} at $T = 1.5$ K shows only one single frequency. (c) Temperature dependence of the relative amplitude of ΔR_{xx} for the sixth Landau level. The solid line is a fit to the Lifshitz–Kosevich formula.[38]

2.3. Shubnikov–de Hass oscillations

Quantum oscillation is a powerful tool to study the electronic properties of materials. It stems from the quantization of Landau levels. In a semiclassical approximation, this results in electrons executing cyclotron orbits confined to quantized Landau tubes. The Landau levels will pass over the Fermi surface one after another as the applied magnetic field is increased, which leads to the density of states oscillating with oscillatory behavior being periodic in inverse magnetic fields. This means that many quantities will exhibit quantum oscillations, since they are functions of the density of states. Various parameters such as electronic spectrum, scattering mechanism, geometry of Fermi surface, etc., can be extracted from the shape, period, and phase of quantum oscillations.[61] Therefore, this technique is widely used to study the electronic properties of materials. For resistance and magnetization, their oscillations are named as Shubnikov–de Hass (SdH) and de Hass–van Alphen (dHvA) oscillations, respectively.

He *et al.* investigated the properties of Fermi surface of Cd_3As_2 by analysing the SdH oscillations at low temperatures.[38] Figure 4(a) shows the oscillatory component ΔR_{xx} versus $1/B$ at various temperatures after subtracting a smooth background. One can see that the oscillations are periodic in $1/B$, as expected from the successive emptying of the Landau levels when the magnetic field is increased. Fast Fourier transform (FFT) method is employed to analyze the frequency of the oscillations, and the result is shown in Fig. 4(b), which consists of only one single frequency $F = 58.3$ T.[38] Therefore, one can directly obtain the Fermi surface area A_F normal to the applied field via the Onsager relation $F = (\Phi_0/2\pi^2)A_F$, where $\Phi_0 = 2.07 \times 10^{-15}$ T·m^2 is the flux quantum. The frequency $F = 58.3$ T corresponds to $A_F = 5.6 \times 10^{-3}$ Å^{-2}.[38] By assuming a circular cross section, a very small Fermi momentum $k_F \approx 0.042$ Å^{-1} is estimated.[38] This result is in good agreement with the ARPES experiment, which gives $k_F \approx 0.04$ Å^{-1}.[29] Note that there are two 3D Dirac points along k_z direction in Brillouin zone, i.e., two Fermi pockets. If the k_F is larger than the distance between the high-symmetry Γ point and Dirac point, these two Fermi pockets will touch each other and the Lifshitz transition (i.e., the Fermi level reaches the valence band top) occurs. Therefore, it is necessary to check whether the Lifshitz transition happens or not. From an ARPES study on a Cd_3As_2 single crystal, the distance between Γ point and Dirac point is about 0.15 Å^{-1}.[27] According to the relation $n_e = k_F^3/3\pi^2$, we can estimate the critical carrier concentration where the Lifshitz transition happens is about 2.4×10^{20} cm^{-3}. Such a value is much larger than our k_F and other works' (Table 1), which means that Cd_3As_2 samples with carrier concentration n_e be-

ing the order of $\sim 10^{18}$ cm^{-3} are not close to the Lifshitz transition. It is worth mentioning that Zhao *et al.* have observed double period oscillations with aligning the magnetic field at certain directions, and they attribute the anomalous oscillation behavior to the Lifshitz transition in their Cd_3As_2 samples.[42]

The SdH oscillation amplitude in Cd_3As_2 can be well described by the Lifshitz–Kosevich formula for a 3D system[61–64]

$$\frac{\Delta\rho_{xx}}{\rho_0} \propto \frac{2\pi^2 k_B T/\hbar\omega_c}{\sinh(2\pi^2 k_B T/\hbar\omega_c)} e^{-2\pi^2 k_B T_D/\hbar\omega_c}, \quad (2)$$

$$R_T = \frac{2\pi^2 k_B T/\hbar\omega_c}{\sinh(2\pi^2 k_B T/\hbar\omega_c)}, \quad (3)$$

$$R_D = e^{-2\pi^2 k_B T_D/\hbar\omega_c}, \quad (4)$$

where ω_c is the cyclotron frequency and T_D is the Dingle temperature. R_T is the thermal damping factor and R_D is the Dingle damping factor. Figure 3(c) shows the temperature dependence of the normalized oscillation amplitude at $1/B = 0.0928$ T^{-1}, which corresponds to the 6th Landau level. Fitting the data by employing Eq. (2), $\hbar\omega_c \approx 24.6$ meV for $n = 6$ can be obtained.[38] For Dirac system, cyclotron frequency ω_c follows the square root dependence on magnetic field.[6,65] By employing $E_n = v_F\sqrt{2e\hbar nB}$ and $v_F = \hbar k_F/m^*$, rather small cyclotron effective mass $m^* \approx 0.044m_0$ and very large Fermi velocity $v_F \approx 1.1 \times 10^6$ m/s are obtained.[38] These values evaluated by transport measurements (Table 1) are consistent with the ARPES and STM results.[27–30] This very large Fermi velocity may explain the unusual high mobility in Cd_3As_2.

2.4. The nontrivial π Berry's phase

Berry's phase is a geometrical phase factor, acquired when quantum mechanical systems adiabatically evolute on a closed path in parameter space.[66,67] A nontrivial or nonzero Berry's phase could result in plenty of emergent phenomena, such as the anomalous and quantum Hall effects,[68,69] and topological insulating and superconducting phases.[3] A distinguished feature of Dirac fermions is that they carry the nontrivial π Berry's phase because the electron orbits enclose a single Dirac point.[70–74] This nontrivial π Berry's phase can be experimentally accessed by analyzing the SdH oscillations, which has been successfully detected in graphene,[73,74] elemental bismuth,[75] the bulk Rashba semiconductor BiTeI,[64] and bulk $SrMnBi_2$.[76] However, situations have become complicated in topological insulators because of the large Zeeman energy effects and bulk conduction.[77–79]

In general, any closed cyclotron orbit is quantized under an applied magnetic field, and can be described by the Lifshitz–Onsager quantization rule

$$A_F\frac{\hbar}{eB} = 2\pi(n + 1/2 + \beta + \delta), \quad (5)$$

where A_F is the extremal cross-sectional area of the Fermi surface related to the Landau level n; $2\pi\beta$ is the Berry's phase, and δ is an additional phase shift resulting from the curvature of the Fermi surface in the third direction, taking the value $\delta = 0$ and $\pm 1/8$ for the 2D and 3D, respectively.[64,65,80] Therefore, to obtain the value of Berry's phase, one can plot the index field $1/B$ versus the Landau index and track the intercept in the limit $B \to \infty$. For the trivial parabolic dispersion in conventional metals, the Berry's phase should be zero; for Dirac systems with linear dispersion, there should be a nontrivial π Berry's phase because the zeroth Landau level is pinned to the Dirac point.[71–74]

He *et al.* have firstly reported that the nontrivial π Berry's phase exists in Cd_3As_2 by means of analysing the SdH oscillations.[38] The Landau index plot of Cd_3As_2 single crystals is presented in Fig. 5.[38] The data points from two Cd_3As_2 single crystals fall into two straight lines, and the linear extrapolation gives the intercepts 0.58 ± 0.01 and 0.56 ± 0.03, respectively.[38] This is a strong evidence for the existence of Dirac fermions in Cd_3As_2 from the bulk transport measurements. The slight deviations from 1/2 indicate the additional phase shifts $\delta \approx 0.08$ and 0.06, which may result from the 3D nature of the Fermi surface of Cd_3As_2.[39–41,64] The existence of the nontrivial Berry's phase has been verified by some other measurements of SdH[41–44,46] and dHvA[43] oscillations, which are presented in Fig. 6. Therefore, complementary to surface-sensitive ARPES[27–29] and STM[30] experiments, the bulk transport measurement results confirm the 3D DSM phase in Cd_3As_2.

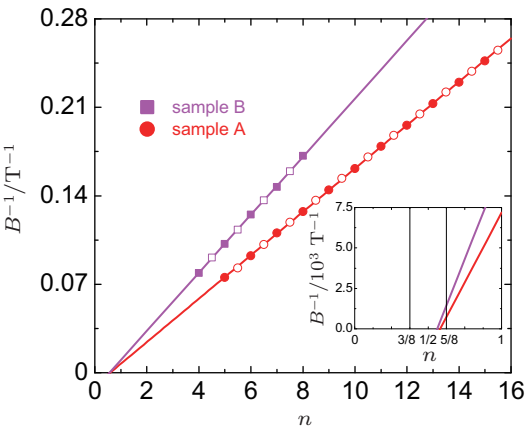


Fig. 5. (color online) Landau index n plotted against $1/B$ for Cd_3As_2 single crystals.[38] The closed circles denote the integer index (ΔR_{xx} valley), and the open circles indicate the half integer index (ΔR_{xx} peak). Two straight-line fittings extrapolate to 0.58 ± 0.01 and 0.56 ± 0.03, respectively, which is a strong evidence for the nontrivial π Berry's phase of 3D Dirac fermions in Cd_3As_2.[38]

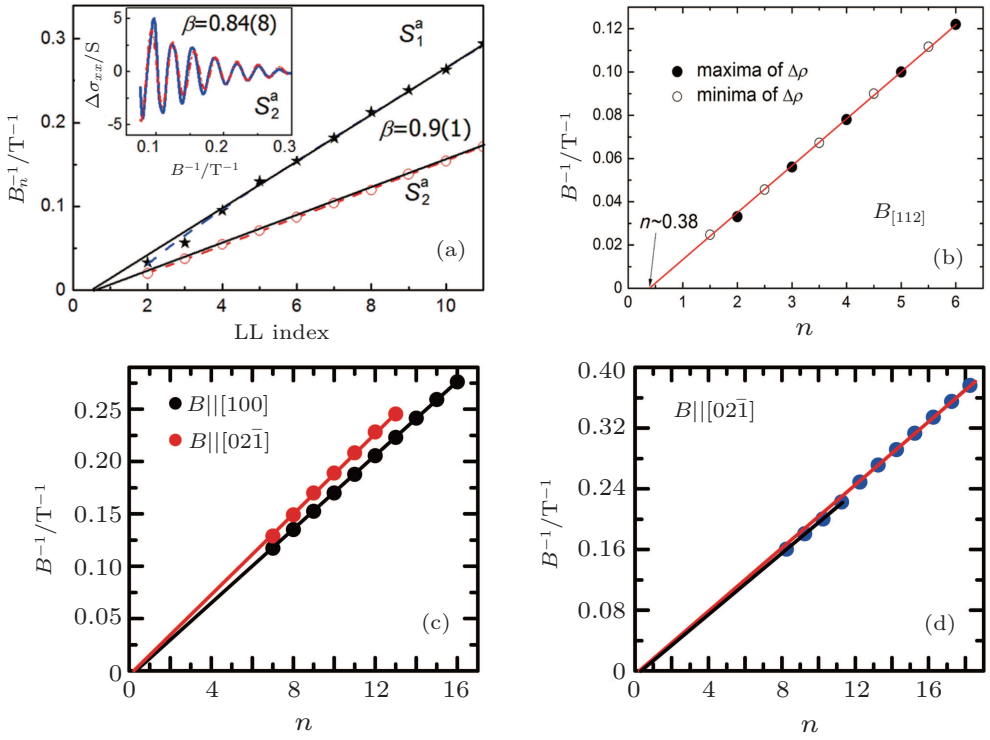


Fig. 6. (color online) The existence of the nontrivial Berry's phase in Cd_3As_2 has been verified by several other measurements of SdH[41–44,46] and dHvA[43] oscillations. For example, the Landau plots in panels (a) and (b) come from the SdH oscillations measured by Narayanan *et al.*[41] and Zhao *et al.*,[42] respectively; (c) and (d) come from the dHvA oscillations measured by Pariari *et al.*[43]

2.5. Evolution of the Berry's phase

One important thing is that once the rotational symmetry of the crystal structure is broken, the 3D Dirac points in Cd_3As_2 are no longer preserved and a mass term will be introduced.[5,6,30] In this situation, a Dirac gap will open at the Dirac points, which means that the nontrivial Berry's phase is no longer π constantly and will turn into a function of the induced mass term.[81] Therefore, if the gap is wide enough, the nontrivial Berry's phase will reduce to zero.[46,81] Actually, a magnetic field whose orientation deviates from the k_z direction would break the rotational symmetry in Cd_3As_2, and induce a small gap.[30] In our electric transport measurements, the external fields are fixed along the (112) direction, and this leads to a gap opening at the Dirac points.[30] However, according to Jeon *et al.*, this Dirac gap is only about 8 meV (at 14.5 T in our measurements).[30] Such a small gap could not affect the value of Berry's phase significantly.[30,81] That is why the nontrivial Berry's phase is still detected in most of quantum oscillation experiments with magnetic field along the (112) direction.[38,41,44,46,81] In this sense, it will be interesting to investigate the evolution of Berry's phase with the magnetic fields and the tilt angles.

Cao *et al.* discovered that the value of the Berry's phase changes with increasing magnetic field.[44] They found that fitting higher magnetic field regimes would give a lower value of Berry's phase when the orientation of the field is perpendicular to (112) direction.[44] Furthermore, the Berry's phase also manifests an angular dependence at different magnetic field regimes.[44] Their results are reproduced in Fig. 7, which are consistent with the theoretical prediction.[5,6,30] They proposed that these changes of the Berry's phase suggest a possible topological phase transition.[44]

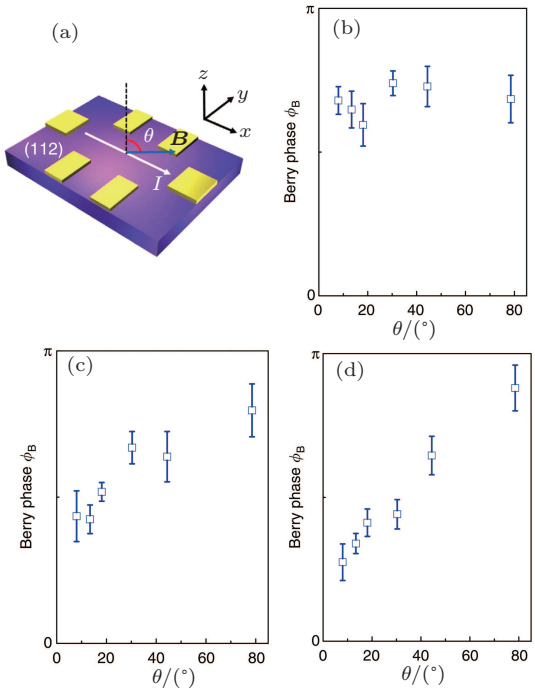


Fig. 7. (color online) (a) Schematic sketch of the magnetoresistance measurements in Ref. [44]. The Berry's phase was fitted in the regimes of (b) 5–7 T (corresponding to ninth to eleventh Landau levels); (c) 7–10 T (seventh to ninth Landau levels); and (d) 10–15 T (fifth to seventh Landau levels).[44] They proposed that these changes of the Berry's phase suggest a field-induced topological phase transition.[44]

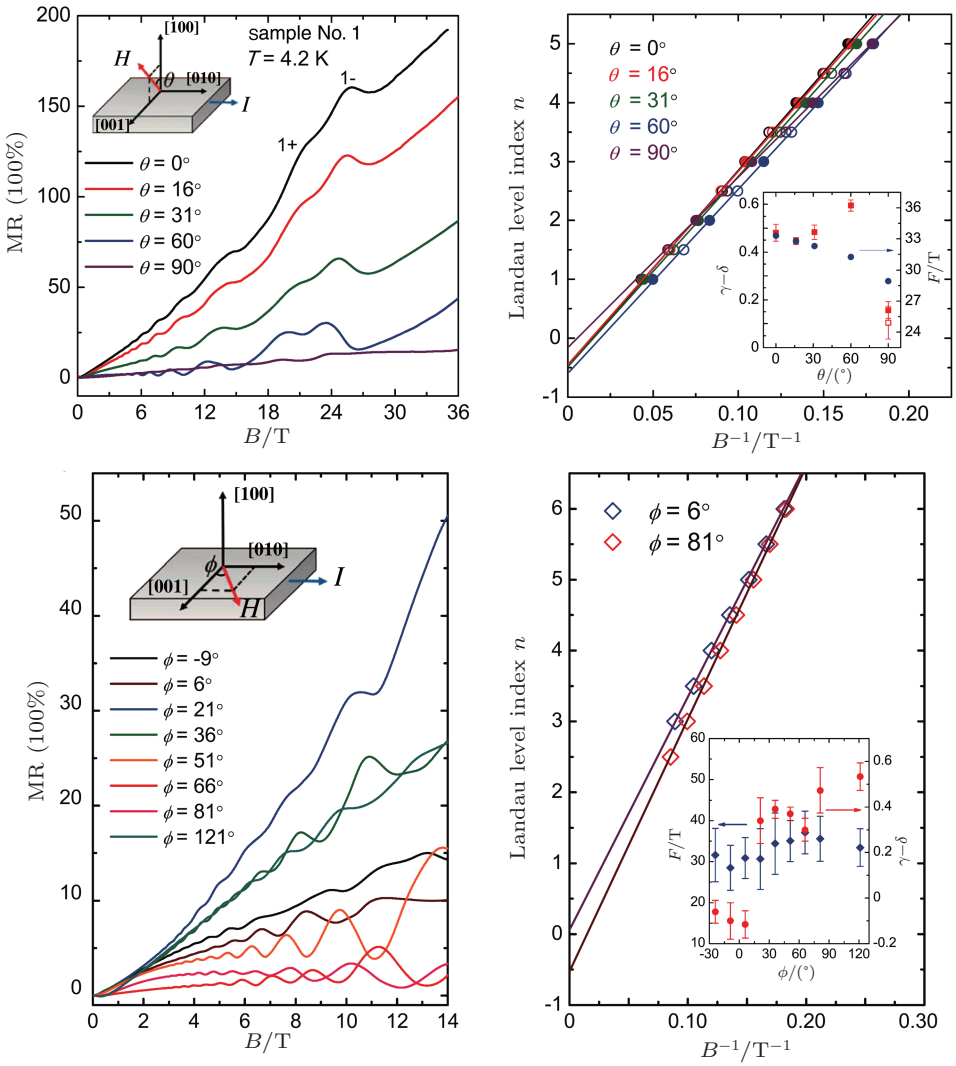


Fig. 8. (color online) (a) Angular dependence of the transverse magnetoresistance with magnetic field rotated in the (010) plane.[46] (b) Angular dependence of the values of the Berry's phase with magnetic field rotated in the (010) plane.[46] (c) Angular dependence of the transverse magnetoresistance with magnetic field rotated in the (100) plane.[46] (d) Angular dependence of the values of the Berry's phase with magnetic field rotated in the (100) plane.[46]

Xiang *et al.* investigated the angular dependence of the Berry's phase thoroughly, and discovered that it can be continuously tuned by the orientation of the magnetic field.[46] In their measurements, the current is along the [010] direction and the external field rotates from [100] to [001] direction.[46] They found that the value of the Berry's phase clearly deviates from 0 when the magnetic field is tilted away by 60 degrees from the initial [100] direction,[46] and finally reaches $\sim \pi$ at [001] direction.[46] Meanwhile, when the external field rotates in the *ab* plane, similar result is also obtained.[46] These results are reproduced in Fig. 8. They proposed that this shift of $\sim \pi$ of the Berry's phase may also hint at a possible topological phase transition induced by a magnetic field tilted away from the high-symmetry direction.[46]

3. Summary

In summary, we have briefly reviewed the quantum transport properties of the three-dimensional Dirac semimetal Cd_3As_2 single crystals, including the unexpected ultra-high charge mobility, large linear magnetoresistivity, remarkable SdH oscillations, nontrivial Berry's phase, and the evolution of the nontrivial Berry's phase. These unusual transport results are related to the novel electronic properties of Cd_3As_2. Moreover, because its Fermi surfaces only consist of 3D Dirac fermions, Cd_3As_2 single crystals or its other structures may have a huge potential for future device applications.

Acknowledgements

We thank P. S. Wang for band structure calculations and Z. J. Xiang for helpful discussions.

References

[1] Geim A K and Novoselov K S 2007 *Nat. Mater.* **6** 183
[2] Castro Neto A H, Guinea F, Peres N M R, Novoselov K S and Geim A K 2009 *Rev. Mod. Phys.* **81** 109
[3] Hasan M Z and Kane C L 2010 *Rev. Mod. Phys.* **82** 3045
[4] Qi X L and Zhang S C 2011 *Rev. Mod. Phys.* **83** 1057

[5] Wang Z, Sun Y, Chen X Q, Franchini C, Xu G, Weng H, Dai X and Fang Z 2012 *Phys. Rev. B* **85** 195320
[6] Wang Z, Weng H, Wu Q, Dai X and Fang Z 2013 *Phys. Rev. B* **88** 125427
[7] Young S M, Zaheer S, Teo J C Y, Kane C L, Mele E J and Rappe A M 2012 *Phys. Rev. Lett.* **108** 140405
[8] Yang B J and Nagaosa N 2014 *Nat. Commun.* **5** 4898
[9] Vafek O and Vishwanath A 2014 *Annu. Rev. Condens. Matter Phys.* **5** 83
[10] Neupane M, Xu S Y, Alidoust N, Sankar R, Belopolski I, Sanchez D S, Bian G, Liu C, Chang T R, Jeng H T, Wang B K, Chang G, Lin H, Bansil A, Chou F and Hasan M Z 2015 *Phys. Rev. B* **91** 241114
[11] Yi H, Wang Z, Chen C, Shi Y, Feng Y, Liang A, Xie Z, He S, He J, Peng Y, Liu X, Liu Y, Zhao L, Liu G, Dong X, Zhang J, Nakatake M, Arita M, Shimada K, Namatame H, Taniguchi M, Xu Z, Chen G, Dai X, Fang Z and Zhou X J 2014 *Sci. Rep.* **4** 6106
[12] Kobayashi S and Sato M 2015 *Phys. Rev. Lett.* **115** 187001
[13] Wan X G, Turner A M, Vishwanath A and Savrasov S Y 2011 *Phys. Rev. B* **83** 205101
[14] Steinberg J, Young S M, Zaheer S, Kane C L, Mele E J and Rappe A M 2014 *Phys. Rev. Lett.* **112** 036403
[15] Koshino M and Ando T 2010 *Phys. Rev. B* **81** 195431
[16] Abrikosov A A 1998 *Phys. Rev. B* **58** 2788
[17] Abrikosov A A 2000 *Europhys. Lett.* **49** 789
[18] Burkov A A, Hook M D and Balents L 2011 *Phys. Rev. B* **84** 235126
[19] Aji V 2012 *Phys. Rev. B* **85** 241101
[20] Son D T and Spivak B Z 2013 *Phys. Rev. B* **88** 104412
[21] Parameswaran, Grover T, Abanin D A, Pesin D A and Vishwanath A 2014 *Phys. Rev. X* **4** 031035
[22] Liu C X, Zhang H J, Yan B H, Qi X L, Frauenheim T, Dai X, Fang Z and Zhang S C 2010 *Phys. Rev. B* **81** 041307
[23] Hosur P, Dai X, Fang Z and Qi X L 2014 *Phys. Rev. B* **90** 045130
[24] Yang S A, Pan H and Zhang F 2014 *Phys. Rev. Lett.* **113** 046401
[25] Liu Z K, Zhou B, Zhang Y, Wang Z J, Weng H M, Prabhakaran D, Mo S K, Shen Z X, Fang Z, Dai X, Hussain Z and Chen Y L 2014 *Science* **343** 864
[26] Xu S Y, Liu C, Kushwaha S K, Chang T R, Krizan J W, Sankar R, Polley C M, Adell J, Balasubramanian T, Miyamoto K, Alidoust N, Bian G, Neupane M, Belopolski I, Jeng H T, Huang C Y, Tsai W F, Lin H, Chou F C, Okuda T, Bansil A, Cava R J and Hasan M Z 2013 arXiv:1312.7624
[27] Liu Z K, Jiang J, Zhou B, Wang Z J, Zhang Y, Weng H M, Prabhakaran D, Mo S K, Peng H, Dudin P, Kim T, Hoesch M, Fang Z, Dai X, Shen Z X, Feng D L, Hussain Z and Chen Y L 2014 *Nat. Mater.* **13** 667
[28] Neupane M, Xu S Y, Sankar R, Alidoust N, Bian G, Liu C, Belopolski L, Chang T R, Jeng H T, Lin H, Bansil A, Chou F and Hasan M Z 2014 *Nat. Commun.* **5** 3786
[29] Borisenko S, Gibson Q, Evtushinsky D, Zabolotnyy V, Büchner B and Cava R J 2014 *Phys. Rev. Lett.* **113** 027603
[30] Jeon S, Zhou B B, Gyenis A, Feldman B E, Kimchi I, Potter A C, Gibson Q D, Cava R J, Vishwanath A and Yazdani A 2014 *Nat. Mater.* **13** 667
[31] Xu S Y, Liu C, Kushwaha S K, Sankar R, Krizan J W, Belopolski I, Neupane M, Bian G, Alidoust N, Chang T R, Jeng H T, Huang C Y, Tsai W F, Lin H, Shibayev P P, Chou F C, Cava R J and Hasan M Z 2015 *Science* **347** 294
[32] Aggarwal L, Gaurav A, Thakur G S, Haque Z, Ganguli A K and Sheet G 2015 *Nat. Mater.* **15** 32
[33] Wang H, Wang H C, Liu H W, Lu H, Yang W H, Jia S, Liu X J, Xie X C, Wei J and Wang J 2015 *Nat. Mater.* **15** 38
[34] He L P, Jia Y T, Zhang S J, Hong X C, Jin C Q and Li S Y 2016 *npj Quantum Materials* **1** 16014
[35] Li C Z, Wang L X, Liu H W, Wang J, Liao Z M and Yu D P 2015 *Nat. Commun.* **6** 10137.
[36] Li H, He H T, Lu H Z, Zhang H C, Liu H C, Ma R, Fan Z Y, Shen S Q and Wang J N 2016 *Nat. Commun.* **7** 10301
[37] Wang L X, Li C Z, Yu D P and Liao Z M 2016 *Nat. Commun.* **7** 10769
[38] He L P, Hong X C, Dong J K, Pan J, Zhang Z, Zhang J and Li S Y 2014 *Phys. Rev. Lett.* **113** 246402
[39] Liang T, Gibson Q, Ali M N, Liu M H, Cava R J and Ong N P 2015 *Nat. Mater.* **14** 280
[40] Feng J, Pang Y, Wu D, Wang Z, Weng H M, Li J, Dai X, Fang Z, Shi Y and Li L 2015 *Phys. Rev. B* **92** 081306
[41] Narayanan A, Watson M D, Blake S F, Chen Y L, Prabhakaran D, Yan B, Bruyant N, Drigo L, Mazin I I, Felser C, Kong T, Canfield P C and Coldea A I 2015 *Phys. Rev. Lett.* **114** 117201
[42] Zhao Y, Liu H, Zhang C, Wang H, Wang J, Lin Z, Xing Y, Lu H, Liu J, Wang Y, Jia S, Xie X C and Wang J 2015 *Phys. Rev. X* **5** 031037
[43] Pariari A, Dutta P and Mandal P 2015 *Phys. Rev. B* **91** 155139
[44] Cao J, Liang S, Zhang C, Liu Y, Huang J, Jin Z, Chen Z G, Wang Z, Wang Q, Zhao J, Li S Y, Dai X, Zou J, Xia Z, Li L and Xiu F 2015 *Nat. Commun.* **6** 7779
[45] Xiong J, Kushwaha S, Krizan J, Liang T, Cava R J and Ong N P 2015 *Science* **350** 413
[46] Xiang Z J, Zhao D, Jin Z, Shang C, Ma L K, Ye G J, Lei B, Wu T, Xia Z C and Chen X H 2015 *Phys. Rev. Lett.* **115** 226401
[47] Zhang S, Wu Q, Schoop L, Ali M N, Shi Y, Ni N, Gibson Q, Sidorov V, Yi W, Guo J, Zhou Y, Gao P, Gu D, Zhang C, Jiang S, Yang K, Li A, Li Y, Li X, Liu J, Dai X, Fang Z, Cava R J, Sun L L and Zhao Z X 2015 *Phys. Rev. B* **91** 165133
[48] Ali M N, Gibson Q, Jeon S, Zhou B B, Yazdani A and Cava R J 2014 *Inorg. Chem.* **53** 4062
[49] Lovett D R 1972 *J. Mater. Sci.* **7** 388
[50] Kloc K and Zdanowicz W 1984 *J. Cryst. Growth* **66** 451
[51] Steigmann G A and Goodyear J 1968 *Acta Cryst. B* **24** 1062
[52] Radautsan S I, Arushanov E K and Chuiko G P 1973 *Phys. Status Solidi A* **20** 221
[53] Jay-Gerin J P, Aubin M J and Caron L G 1977 *Solid State Commun.* **21** 771
[54] Zdanowicz L, Portal J C and Zdanowicz W 1983 *Lect. Notes Phys.* **177** 386
[55] Parish M M and Littlewood P B 2003 *Nature* **426** 162
[56] Parish M M and Littlewood P B 2005 *Phys. Rev. B* **72** 094417
[57] Hu J S, Parish M M and Rosenbaum T F 2007 *Phys. Rev. B* **75** 214203
[58] Zhang W, Yu R, Feng W, Yao Y, Weng H, Dai X and Fang Z 2014 *Phys. Rev. Lett.* **106** 156808
[59] Friedman A L, Tedesco J L, Campbell P M, Culbertson J C, Aifer E, Perkins F K, Myers-Ward R L, Hite J K, Eddy Jr. C R, Jernigan G G and Gaskill D K 2010 *Nano Lett.* **10** 3962
[60] Hu J S and Rosenbaum T F 2008 *Nat. Mater.* **7** 697
[61] Shoenberg D 1984 *Magnetic oscillations in metals* (Cambridge Univ. Press).
[62] Roth L M and Argyres P N 1966 *Semiconductors and Semimetals* (New York: Academic Press) pp. 159–202
[63] Rashba E I and Landwehr G 1991 *Landau Level Spectroscopy: Modern Problems in Condensed Matter Sciences* (Amsterdam: North-Holland) vol. 27.2.
[64] Murakawa H, Bahramy M S, Tokunaga M, Kohama Y, Bell C, Kaneko Y, Nagaosa N, Hwang H Y and Tokura Y 2013 *Science* **342** 1490
[65] Luk'yanchuk I A and Kopelevich Y 2004 *Phys. Rev. Lett.* **93** 166402
[66] Berry M V 1984 *Proc. R. Soc. Lond. A: Math. Phys. Sci.* **392** 45
[67] Xiao D, Chang M C and Niu Q 2010 *Rev. Mod. Phys.* **82** 1959
[68] Nagaosa N, Sinova J, Onoda S, MacDonald A H and Ong N P 2010 *Rev. Mod. Phys.* **82** 1539
[69] Thouless D J, Kohmoto M, Nightingale M P and den Nijs M 1982 *Phys. Rev. Lett.* **49** 405
[70] Ando T, Nakanishi T and Saito R 1998 *J. Phys. Soc. Jpn.* **67** 2857
[71] Mikitik G P and Sharlai Y V 1999 *Phys. Rev. Lett.* **82** 2147
[72] Mikitik G P and Sharlai Y V 2004 *Phys. Rev. Lett.* **93** 106403
[73] Novoselov K S, Geim A K, Morozov S V, Jiang D, Katsnelson M I, Grigorieva I V, Dubonos S V and Firsov A A 2005 *Nature* **438** 197
[74] Zhang Y B, Tan Y W, Stormer H L and Kim P 2005 *Nature* **438** 201
[75] Zhu Z W, Fauqué B, Fuseya Y and Behnia K 2011 *Phys. Rev. B* **84** 115137
[76] Park J, Lee G, Wolff-Fabris F, Koh Y Y, Eom M J, Kim Y K, Farhan M A, Jo Y J, Kim C, Shim J H and Kim J S 2011 *Phys. Rev. Lett.* **107** 126402
[77] Qu D X, Hor Y S, Xiong J, Cava R J and Ong N P 2010 *Science* **329** 821
[78] Analytis J G, McDonald R D, Riggs S C, Chu J H, Boebinger G S and Fisher I R 2010 *Nat. Phys.* **6** 960
[79] Sacépé B, Oostinga J B, Li J, Ubaldini A, Couto N J G, Giannini E and Morpurgo A F 2011 *Nat. Commun.* **2** 575
[80] Luk'yanchuk I A and Kopelevich Y 2006 *Phys. Rev. Lett.* **97** 256801
[81] Wright A R and McKenzie R H 2013 *Phys. Rev. B* **87** 085411